Surface and Subsurface Hydrodynamics of Inland Wetlands in Brazil: Integrating High-Resolution Remote Sensing and Hydrogeophysics

Lucas Moreira Furlan [1], César Augusto Moreira [2], Vânia Silvia Rosolen [3]

[1] São Paulo State University, Department of Geology, Laboratory of Geospatial Technologies, Rio Claro, São Paulo, Brazil – lucas.m.furlan@unesp.br

[2] São Paulo State University, Department of Geology, Rio Claro, São Paulo, Brazil – cesar.a.moreira@unesp.br

[3] São Paulo State University, Department of Environmental Engineering, Rio Claro, São Paulo, Brazil – vania.rosolen@unesp.br

Keywords: Unmanned aerial vehicle, 3D hydrogeophysics, 3D surface water paths, Savanna.

Abstract

Inland wetlands, especially those isolated from surface water systems, present complex hydrological dynamics due to interactions between meteoric water, soil moisture, and groundwater. These ecosystems act as critical zones of recharge and discharge within a catchment, and their balance is increasingly disturbed by land use changes and climate variability. The challenge is even greater in isolated wetlands, where the absence of visible surface connectivity complicates the understanding of their hydrological role—particularly in regions subjected to seasonal heavy rainfall and high evapotranspiration. To overcome these challenges, this study applies an integration of high-resolution remote sensing and hydrogeophysical techniques to develop 3D surface and subsurface hydrological models. These tools allow detailed spatial analysis of terrain morphology, soil saturation zones, and subsurface water pathways, thereby enhancing the characterization of wetland structure and function. The surface modelling component utilizes drone imagery to delineate microtopography and surface flow patterns, while subsurface modelling incorporates geophysical surveys (electrical resistivity tomography) to map below-ground water distribution and interactions with soil and aquifers. This multidisciplinary approach offers insights into the water storage capacity and connectivity of wetlands, contributing to a more robust understanding of their ecological and hydrological significance.

1. Introduction

Human well-being is closed related to the maintenance of ecosystem services, and water is one of the most important. Water scarcity and hydric vulnerability are increasing due to frequent extreme droughts and intensified land use conversion. This issue is more severe in developing countries, where the risk is up to five times higher than the rest of the world (Esfahanian et al., 2017, Tabari et al., 2021). Traditionally, water supply claims focus on guaranteeing a specific volume and quality at a given time. However, other factors related to hydrological services, such as the location and timing of flow as water moves through the landscape, are often undervalued (Brauman et al, 2007). The pattern of water distribution is affected by ecosystem heterogeneity, while land use land cover (LULC) affects particularly the water storage (Guo and Gan, 2003, Steele and Heffernan, 2014). Geographically isolated wetlands (GIWs) are environments recognized for providing a wide range of ecosystem services, including the enhancement of watershed biodiversity, biogeochemical cycling, and the storage and recharge of water supplies (Leibowitz, 2003).

The complexity of GIWs in retaining rainwater and connecting to surface water systems through shallow or deep aquifer flows, surface runoff, or shallow subsurface flows necessitates the use of a hydrological model with appropriate parameterization and calibration. This approach is essential for developing scenarios that characterize the presence of GIWs in a landscape (Golden et al., 2014). However, the hydrology of GIWs is significantly degraded when surrounded by agriculture with inadequate management as this activity consumes large amounts of water and is central to water-related risks and vulnerabilities (OECD, 2023).

The exchange of water among wetlands, surface water, and groundwater varies over space and time. In catchments dominated by intensive agriculture, the variability can harm the system's integrity, contributing to wetland loss and causing widespread hydrological and ecological imbalances (Winter, 2007; Zedler, 2003; Bruland et al., 2003; McLaughlin et al., 2014).

Brazil has been facing extremely hot summers, with increasingly frequent and severe heat waves and changes in the precipitation pattern. In August 2024, 200 municipalities experienced extreme drought conditions, including 82 municipalities in the state of São Paulo and several cities in the Amazon and Central regions, which had gone up to 12 months without rain (CEMADEN/MCTI, 2024).

Water resources management will benefit from encouraging studies on hydrological structural and functional connectivity at multiple scales (Zhang et al., 2021). Geospatial technologies based on high-resolution remote sensing techniques and shallow 3D geophysical surveys can be invaluable tools for management, as they can capture and map the storage and flow of water, including the spatio-temporal connections between surface and shallow-to-deep groundwater (Yáñez-Morroni et al., 2023). The integration of surface and subsurface 3D modelling approach offers a more comprehensive and cost-effective solution for hydrological analysis and prediction. It provides an effective and realistic understanding of hydrology at both surface and subsurface levels, surpassing traditional methods that may rely heavily on predictive statistics alone. Such an approach facilitates deeper insights into hydrological dynamics, which are essential for effective water resource management.

The objective of this study is to propose a geospatial technologies-based method, incorporating 3D surface and subsurface modelling, to deepen the understanding of environmental issues related to water availability in geographically isolated wetlands.

https://doi.org/10.5194/isprs-archives-XLVIII-2-W10-2025-71-2025 | © Author(s) 2025. CC BY 4.0 License.

2. Methodology

2.1 Study Area

The study area, a geographically isolated wetland (Figure 1), is situated in the Corumbataí River Basin within the Paraná Sedimentary Basin. This region's geological composition is diverse, from the Carboniferous to Cretaceous periods. The surface layer is predominantly composed of sandstones from the Rio Claro Formation (Tertiary) and Quaternary period, as well as continental and alluvial deposits (Zaine et al., 2000).

Located in the central-western São Paulo State, Brazil, the study site lies within the *Paulista Peripheral Depression* (PPD), an inland area bordered by a basalt-sandstone cuesta and the Atlantic crystalline plateau (Almeida, 2964). The region experiences a subtropical climate (Cwa type according to Koeppen's classification), with an average temperature of 21.6°C and an annual rainfall of 1,366 mm (CEPAGRI, 2020).

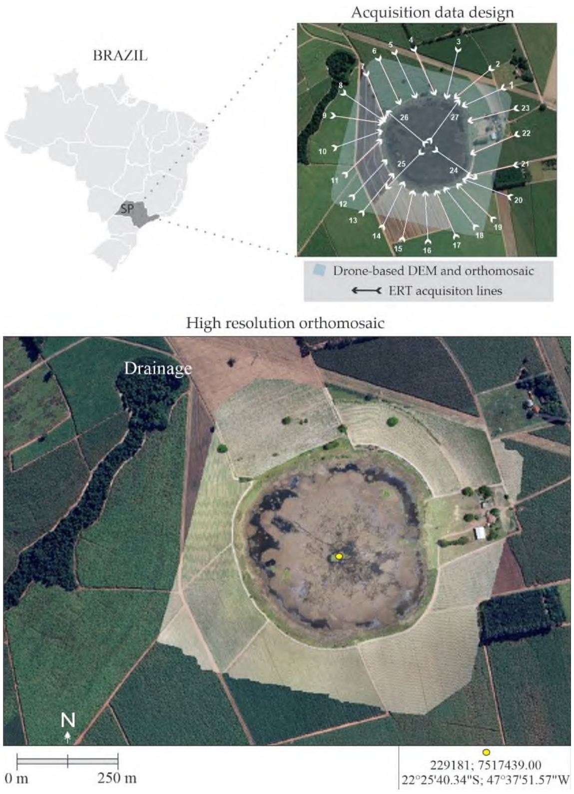

Figure 1. Study area located in São Paulo State, Brazil.

2.2 Drone-based photogrammetry: Surface water flow.

Data were acquired using a DJI Phantom 4 Pro UAV (DJI, 2023). Flights were planned with PIX4D to ensure >80% image overlap (D'Oleire-Oltmanns et al., 2012; Furlan et al., 2023). Images captured (250 total) were processed using the SfM-MVS technique in Agisoft Metashape to generate DEMs and orthomosaics (Gomez et al., 2015; Agisoft, 2023), with planialtimetric correction via DGPS and GCPs (Collischonn et al., 2015). This technique involves generating a dense point cloud from overlapping 2D images captured by the UAV (SfM) and constructing a 3D mesh using vertices and polygons (MVS) (Gomez et al., 2015). Resulting data (3.44 cm/pixel resolution) were analyzed in Global Mapper 21.0 to simulate surface flow and delineate micro-watersheds and drainage networks (Furlan et al., 2021). The software employs the eight-direction pour point algorithm (D-8) for determining the flow direction at each location. This method includes a bottom-up approach for ascertaining flow direction across flat terrains and incorporates a custom algorithm designed to automatically rectify depressions in the terrain data (DEM). The outcomes of this simulation were instrumental in generating two key maps: first, the delineation of micro watershed areas, consisting of 7191 distinct features; and second, a detailed stream network complemented by drainage areas for each stream segment, encompassing a total of 6096 features.

2.3 DC Resistivity: 3D Hydrogeophysics

Hydrogeophysics using DC Resistivity was applied to investigate the shallow subsurface, as this method effectively detects variations in geological materials and moisture content based on electrical resistivity (Kearey et al., 2002; Milson, 2003). The lateral distribution of electrical resistivity data in the subsurface is ascertained by interpolating discrete spatial data to create bidimensional sections acquired by Electric Resistivity Tomography (ERT) lines, which can further be interpolated to form a 3D block representation of the subsurface. The initial field data represent apparent electrical resistivity, as they are weighted arithmetic means influenced by the electrical current flowing through various geological materials in the subsurface.

The equipment employed in this study was the Resistivity Meter Swedish Terrameter LS from ABEM (Sweden), designed for automatic acquisitions based on pre-set configurations. Its specifications include 84 channels, a 250W power capacity, a maximum current output of 2.5A, and a resolution of 1mV (ABEM, 2012). The acquisition involved 27 ERT lines, each extending 200 meters, resulting in a total of 5400 linear meters of acquisition and 5805 measures of electric resistivity. The layout encompassed the centre and surroundings of the wetland. The Schlumberger array, which entails arranging four electrodes in a straight line with equal spacing, was used for acquisition, with the outer electrodes facilitating current injection and the inner electrodes measuring voltage. Data processing was carried out using Res2Dinv software, focusing on the generation of 2D inversion models. The interpolation and inversion of data are grounded in the Ordinary Least Squares (OLS) mathematical model, which aids in smoothing extreme values and minimizing discrepancies between measured and modelled electrical resistivity values. The quality of the final model was assessed using the Root-Mean-Squared (RMS) parameter, which quantifies the agreement between the calculated inversion model and the field data, in addition to identifying the presence of extreme values (Loke and Barker, 1996).

The 3D block model was processed using the Oasis Montaj platform (Geosoft, 2014). Each numerical output from the 2D inversion model was integrated into a single worksheet. This integration of the 27 lines yielded a comprehensive 3D model, which can be visualized in slices at varying depths of 5 meters each.

3. Results and Discussion

In the study area, the lack of visible surface water connectivity and the extensive landscape transformation due to significant Land Use Land Cover (LULC) changes make it unclear how large the GIW buffer is. When the surface connection between GIWs and rivers is not discernible, the causal relationship between hydrology and geomorphology becomes obscured. This complicates the establishment of buffer strips between water bodies, which are essential for restoring impacted environments and managing water resources (Sidle et al., 2017).

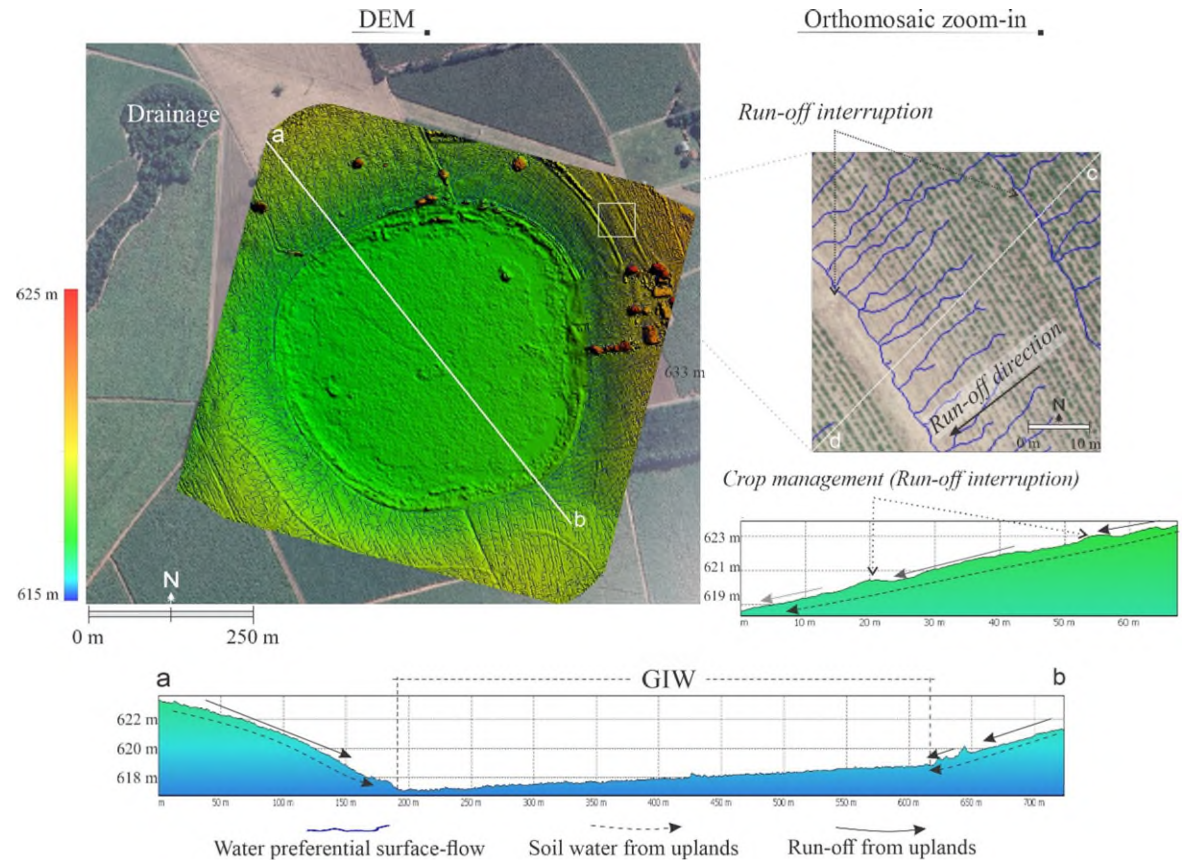

Figure 2. High-Resolution Drone-Based Digital Elevation Model (DEM) superimposed on a Maxar Technologies satellite image, highlighting the drainage in the northwest. This post-processed DEM illustrates the surface water flow across the entire contributing area of the wetland. Elevation profile a-b shows the position of the GIW, situated lower than its contributing area, and outlines the soil water flows and run-off from the uplands. Zoomed-in section of the high-resolution orthomosaic reveals preferential water flow paths and indicates the flows disruptions caused by sugarcane crop management. Elevation profile c-d demonstrates the flow directions in this specific area.

Considering the absence of a buffer zone in our study site, simulations were conducted in and around the wetland, providing accurate spatio-temporal information about the water flow paths generated by the agricultural management practices (Figure 2). This procedure was effective due to the acquisition of very high-resolution UAV imagery, as most freely available satellite images are unable to capture small wetlands (<10 hectares) or account for seasonal variations (Furlan et al., 2023; Junqueira et al., 2024).

In the photogrammetric drone-based 3D data, it was identified that the area surrounding the GIW was dominated by plowed soil. The preferential surface water flow path was automatically traced over this area, overlapping with erosive interrill and rill features primarily created by the machinery used during various stages of sugarcane management. These scars serve as preferential pathways for water flow, converging from the slope towards the wetland. This type of accelerated erosion is commonly observed in sugarcane cultivation over the most erodible Brazilian soils (e.g., Ultisols and Oxisols), which are characterized by a dominance of fine sand fractions (Thomaz et al., 2022), as found in the study area. Several studies have shown that deforestation and land conversion to other uses intensify soil erosion, presenting an alarming problem as erosion degrades soil structure, accelerates the oxidation of organic matter, and disrupts the function of wetlands (Wolka et al., 2015). Water retention in soil is influenced by LULC, which is a significant parameter affecting water resources. To protect the GIW, it is essential to control accelerated erosion in the surrounding areas, as this impacts key hydrological parameters such as evapotranspiration, surface runoff, and groundwater recharge, all of which regulate the water balance across the entire basin (Wojkowski et al., 2023).

Furlan et al. (2023) employed centimetric, very-high-resolution data obtained from drone-based RGB 3D elevation models to evaluate the seasonal dynamics of inundation in the GIW. The peak inundation of the GIW occurred in March, at the end of the rainy season, reaching the border of the wetland. The period of lowest flooding was recorded in October, with a measured retraction of 14,943 m² in surface area at the end of the dry season and the beginning of the wet season during the 2019-2020 period. The hydroperiod was regulated by rainfall, reflecting the well-marked wet and dry seasons, while the depressed topography exerted significant control on water permanence. The results indicate that rainwater accumulates in the GIW and the extent of inundation in this type of wetlands is strongly correlated with the total amount of precipitation.

Previous studies using remote sensing to assess the presence or absence of surface water in GIW over time have demonstrated highly accurate predictions of wet and dry periods, effectively capturing the general patterns and short-term dynamics that are key parameters for wetland function and aquatic life (e.g., Kissel et al., 2020; Chandler et al., 2016; Riley and Stillvell, 2023). In the study of the GIW, it was observed that even under conditions of maximum water level on the topographic surface,

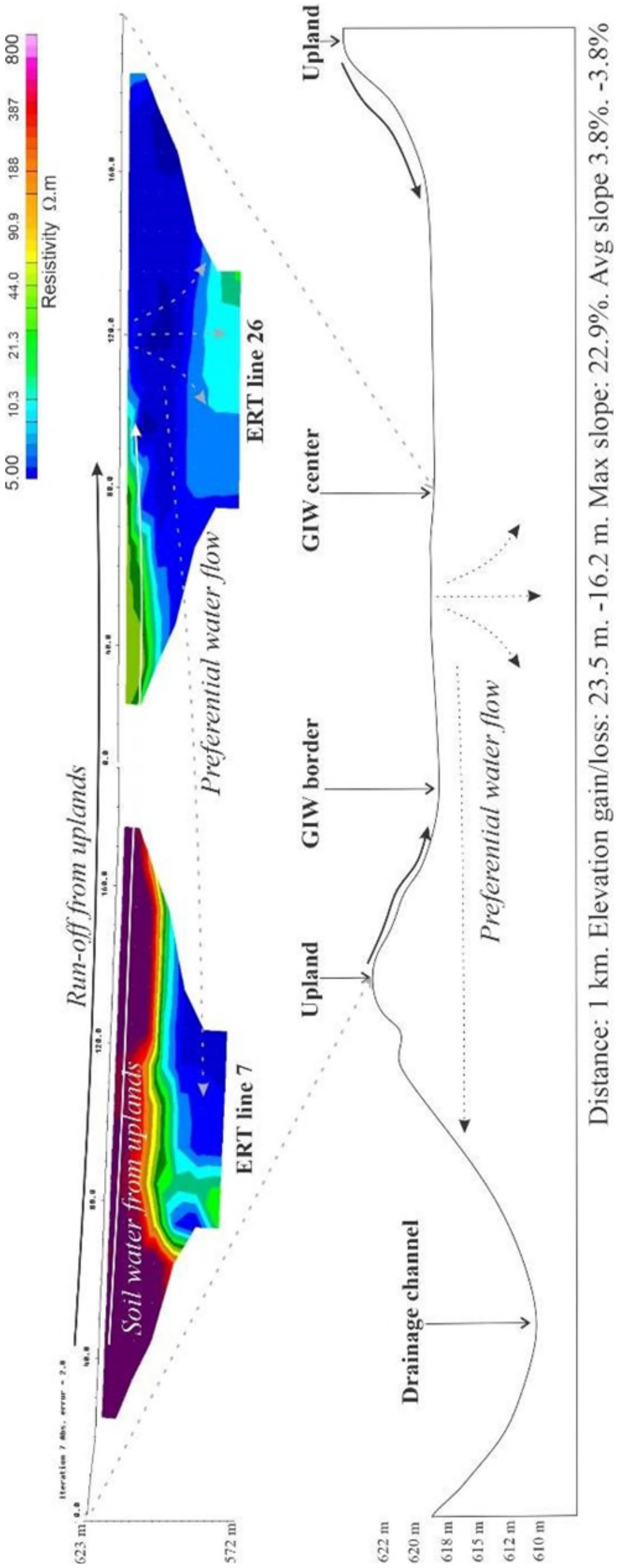

Figure 3. ERT lines 7 (from upland to wetland border) and 26 (from wetland border to wetland centre) were arranged in a continuous transverse sequence. Hot colours indicate high resistivity (indicating less moisture or water content) while cold colours denote low resistivity (implying higher moisture or water content).

no overflow occurred, and surface connectivity between the wetland and downstream water bodies was not apparent.
However, uncertainty remains regarding the connection between surface water, primarily supplied by precipitation, and the aquifer. To investigate this connection between surface and groundwater, DC Resistivity was employed.
The acquisition of ERT lines from upland areas to the center of the wetland indicated that the surrounding areas of the GIW were generally more resistive in the upper layers and less resistive at greater depths. This pattern is probably associated with the occurrence of a shallow aquifer that extends continuously in conjunction with the GIW (Figure 3).

Runoff occurs from the uplands to the wetland border, and soil water flux extends from the uplands to the centre of the wetland. Preferential groundwater flow paths are observed as: i) a slow vertical flow from the entire GIW compartment to deeper sedimentary layers; and ii) a slow horizontal flow from the entire GIW compartment towards the drainage channel. This flow does not represent a significant loss of water, even considering the expected pressure differences due to hydraulic gradient.

The ERT lines were interpolated to create a visual three-dimensional model of the connectivity, extending from the wetland to its surroundings (Figure 4). The three-dimensional DC Resistivity modelling facilitated the delineation of water flow pathways through soil, saprolite, rock, and aquifers, or towards drainage channel. This approach acknowledges that the hydrological complexity in such landscapes is influenced by a variety of factors, including geological settings and hydrological conditions (Neff and Rosenberry, 2018).

The intricate connectivity refers to the genuine interaction between surface water and groundwater, encompassing a system of storage and flux (Winter, 1988). The 3D geophysical model revealed that meteoric water was concentrated in the central compartment of the GIW. This meteoric water, retained in the soil porosity, corresponds to a system whose primary hydrological function is to recharge a shallow aquifer. The water-saturated pores, indicated by lower resistivity values, extend from the soil surface to a depth of 5 meters, reaching the saturated zone at 50 meters. This pattern highlights the direct interaction between the atmosphere, soil, and soil-shallow groundwater, which governs the distribution of water within the wetland.

Comparing the local base level of GIW and the base level of the river channel, the gradient is 8 meters. The local base level of the river is represented by the topographic elevation of 612 m altitude meters while the topographic elevation of GIW is 620 m altitude meters. The GIW is elevated within the catchment while the river incised vertically fitted in a regional-scale fracture. Generally, the river base level controls water connectivity in the catchment (Sidle et al., 2017). However, at the studied site, the deep incision of the river and the hydraulic gradient only facilitate the propagation of water to downstream water bodies from the soil and shallow groundwater. This indicates that the flow pathways never directly connect the wetland water to the drainage network.

The GIW constitutes a confined hydrological compartment where surface water (originating from soil and shallow aquifers) gradually permeates into the deep aquifer through the continuous layers of siltstone and claystone. The geological setting of the area, characterized by notable sedimentary heterogeneity, determines the paths of water flow. In the basin, sedimentary sandy materials predominate in the altimetric positions of the hills, overlying clay formations.

The zone of lower resistivity, encompassing the soil and shallow aquifer (from the surface to a depth of 10 m), is also observed in the northwest section of the maps (Figure 4), extending toward the river channel. However, the pattern of this low resistivity zone does not indicate a significant contribution from both the soil and shallow aquifer to the river flow, as the connectivity is indirect and does not extend upslope to reach the river channel. Lateral subsurface seepage from the wetland appears to be a minor hydrological component in the studied landscape. Some authors have noted that seepage from an isolated wetland can act as a discharge into surface waters in the lower portions of regional flow fields (Pyzoha et al., 2008).

Current land-use and land-cover (LULC) changes have intensified the input of agrochemicals and sediments into wetlands, with agriculture and bare soils serving as major sources of nonpoint source pollution. Fertilizers and pesticides can be adsorbed onto organic matter and mineral particles in hydric soils, posing potential threats to aquatic ecosystems. Wetland soils are particularly effective at retaining nonpoint source pollutants such as nitrogen (N), phosphorus (P), toxic metals, and sediments transported through slope erosion (Kao and Wu, 2001). However, poor land management practices that alter the natural transition between well-drained and poorly drained soils can severely compromise wetland functions (Fensham and Fairfax, 2003).

The widespread presence of agriculture has a substantial negative impact on water volume because intensification leads to increased soil degradation, erosion, and sediment input into the wetland (Ockenden et al., 2014). Our study shows that the land-use pattern results in degradation and loss of the area characterized by GIW, due to the encroachment of upland agriculture towards the wetland's border. Furthermore, soil exposure for a certain period each year, combined with the intensity of precipitation events or droughts, exacerbates runoff and erosional processes on slopes
Integrated 3D surface and subsurface modelling is increasingly essential for understanding the spatial distribution and dynamics of water storage compartments. This approach allows for the representation of complex interactions between surface water bodies, soil moisture zones, and groundwater systems, providing a more realistic and detailed framework for assessing hydrological connectivity in GIW landscapes. By capturing both vertical and lateral fluxes, integrated models enhance our ability to simulate water movement across landscape compartments, informing conservation and management strategies under changing land use and climate conditions.

4. Conclusions

This study highlights the importance of 3D modelling and the integration of surface and subsurface modelling in the investigation of small ecosystems located in environmental risk hotspots. Such ecosystems, often characterized by complex interactions between surface water and groundwater, demand detailed spatial and temporal analysis to fully understand their hydrological and ecological dynamics.

Key findings reveal the intricate connections between hydrogeomorphology and groundwater behavior in a geographically isolated wetlands (GIW). We have elucidated the hydrological dynamics within a small, closed basin characterized by significant sedimentary heterogeneity. The GIW, shaped by topographic depressions and influenced by varying hydroperiods, plays a critical role in the hydrological cycle. The wetland acts as confined hydrological compartments, where surface water from soil and shallow aquifers permeates into deeper strata, influenced by the geological settings.

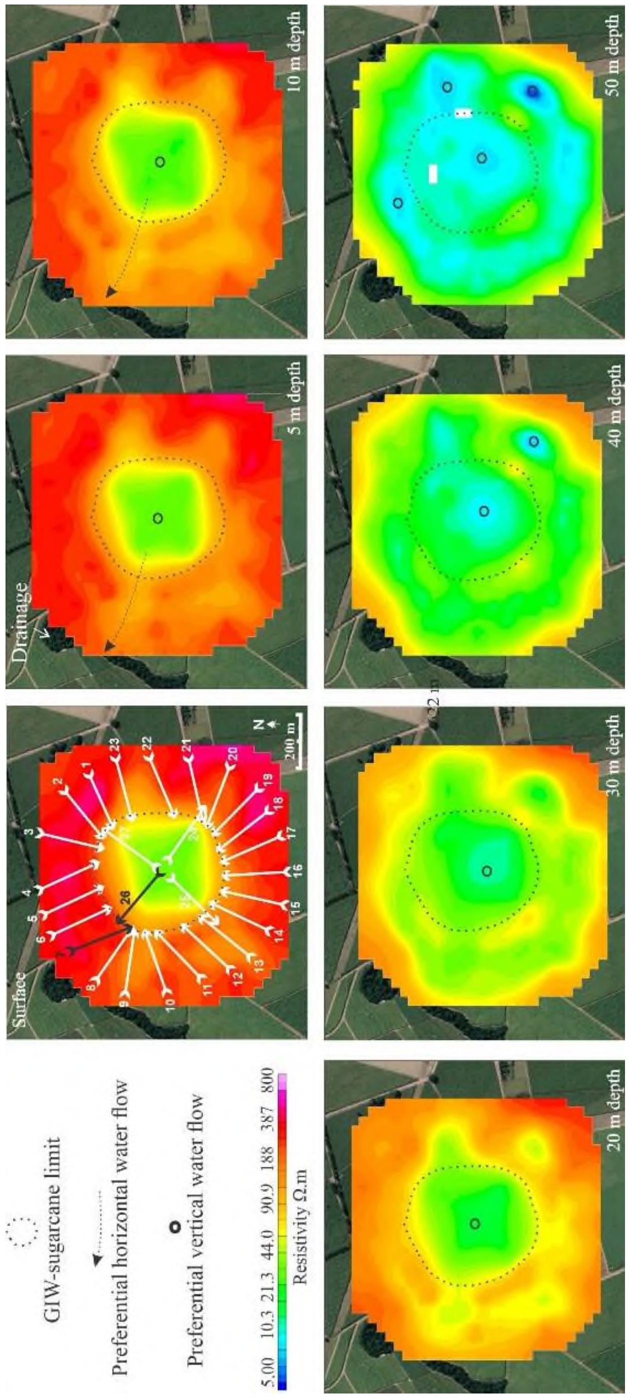

Figure 4. 3D Block-Slices of DC Resistivity at Various Depths (Surface to 50 m depth). Black dotted-arrows show the direction of preferential horizontal groundwater flow, while black circles indicate regions of prominent vertical groundwater flow. This figure visually represents the dynamic interaction between surface and subsurface hydrological processes in the studied area.

This integrated approach is essential for developing effective conservation strategies and managing wetland ecosystems sustainably. The study also demonstrated the vulnerability of these ecosystems to climate change and land-use land-cover (LULC) conversions.

The absence of direct flow towards the streamflow and the deep aquifer indicates that the GIW may not significantly contribute to catchment recharge. However, this area is vital to the catchment's hydrology as a closed, depressed zone that receives convergent flow from the highly weathered soil covering the gentle slopes surrounding the GIW. Since the primary water inputs in the GIW are from precipitation, combined with runoff and seepage from uplands, the GIW is an ecosystem extremely sensitive to and impacted by climate LULC changes.

Acknowledgements

The authors dedicate this work to the memory of our dear colleague, physicist Allan da Silva Tomazella, who made significant contributions at various stages in the development of this project.

This work was funded by the FAPESP - *Fundação de Amparo à Pesquisa do Estado de São Paulo* (Process n. 2020/03207-9 and 2023/04732-8).

References

ABEM, 2012. Terrameter LS: Instruction Manual (ABEM100709).

Agisoft, 2023. Metashape Professional Software, Version 1.6.3. Retrieved November 30, 2023, from https://www.agisoft.com

Almeida, F. F. M., 1964. Geological foundations of São Paulo relief. In *Geology of the State of São Paulo* (pp. 167-263). São Paulo: Geographic and Geological Institute.

Brauman, K. A., Daily, G. C., Duarte, T. K. E., Mooney, H. A., 2007: The nature and value of ecosystem services: an overview highlighting hydrologic services. *Annu. Rev. Environ. Resour.*, 32(1), 67-98.

Bruland, G. L., Hanchey, M. F., & Richardson, C. J., 2003. Effects of agriculture and wetland restoration on hydrology, soils, and water quality of a Carolina bay complex. *Wetlands Ecology and Management,* 11, 141–156.

Cepagri, 2020. Clima dos municípios paulistas. http://www.cpa.unicamp.br *(10 January 2020).*

CEMADEN, 2024. from https://www.gov.br/cemaden/pt-br *(13 January 2025).*

Chandler, H. C., Rypel, A. L., Jiao, Y., Haas, C. A., Gorman, T. A. 2016. Hindcasting historical breeding conditions for an endangered salamander in ephemeral wetlands of the southeastern USA: implications of climate change. *PLoS One,* 11(2), e0150169.

Collischonn, C., de Lima, E. M., Ruiz, L. F. C., Araujo, T. D., Matsuoka, M. T., 201. Posicionamento GNSS: Comparação entre coordenadas oficiais de estações da RBMC e as obtidas por PPP e posicionamento relativo e ajustamento. In *Simpósio Brasileiro de Sensoriamento Remoto*—SBSR. INPE: João Pessoa, Brazil.

D'Oleire-Oltmanns, S., Marzolff, I., Peter, K. D., Ries, J. B., 2012. Unmanned Aerial Vehicle (UAV) for Monitoring Soil Erosion in Morocco. *Remote Sensing,* 4, 3390–3416.

DJI, 2023. Phantom 4PRO. https://www.dji.com/br/phantom-4-pro *(30 November 2024).*

Esfahanian, E., Nejadhashemi, A. P., Abouali, M., Adhikari, U., Zhang, Z., Daneshvar, F., Herman, M. R., 2017. Development and evaluation of a comprehensive drought index. *Journal of Environmental Management*, 185, 31-43.

Fensham, R. J., Fairfax, R. J. 2003. Spring wetlands of the great artesian basin, Queensland, Australia. *Wetlands Ecology and Management*, *11*(5), 343-362.

Furlan, L. M., Ferreira, M. E., Moreira, C. A., de Alencar, P. G., Casagrande, M. F. S., Rosolen, V., 2023. Satellite, UAV, and Geophysical Data to Identify Surface and Subsurface Hydrodynamics of Geographically Isolated Wetlands: Understanding an Undervalued Ecosystem at the Atlantic Forest-Cerrado Interface of Brazil. *Remote Sensing,* 15(7), 1870. https://doi.org/10.3390/rs15071870

Furlan, L. M., Moreira, C. A., de Alencar, P. G., Rosolen, V., 2021. Environmental monitoring and hydrological simulations of a natural wetland based on high-resolution unmanned aerial vehicle data (Paulista Peripheral Depression, Brazil). *Environmental Challenges*, 4, 100146. https://doi.org/10.1016/j.envc.2021.100146

Geosoft, 2014. Oasis Montaj How to Guide. 2014. http://updates.geosoft.com/downloads/files/how-to-guides/Oasis_montaj_Gridding.pdf.

Gomez, C., Hayakawa, Y., Obanawa, H., 2015. A study of Japanese landscapes using structure from motion derived DSMs and DEMs based on historical aerial photographs: New opportunities for vegetation monitoring and diachronic geomorphology. *Geomorphology*, 242, 11–20.

Golden, H. E., Sander, H. A., Lane, C. R., Zhao, C., Price, K., D'Amico, E., Christensen, J. R., 2016. Relative effects of geographically isolated wetlands on streamflow: a watershed-scale analysis. *Ecohydrology*, 9, 21–38.

Guo, Z., Li, Y., Gan, Y., 2003. Spatial pattern of ecosystem function and ecosystem conservation. *Environmental Management*, 32, 682-692.

Kao, C. M., Wu, M. J., 2001. Control of non-point source pollution by a natural wetland. *Water Science and Technology*, *43*(5), 169-174.

Kearey, P., Brooks, M., Hill, I., 2009. *Geofísica de Exploração*. (M. C. M. Coelho, Trans.). São Paulo: Oficina de Textos.

Kissel, A. M., Halabisky, M., Scherer, R. D., Ryan, M. E., Hansen, E. C., 2020. Expanding wetland hydroperiod data via satellite imagery for ecological applications. *Frontiers in Ecology and the Environment*, *18*(8), 432-438.

Koeppen, W., 1948. Climatologia: con un estudio de los climas de la tierra.

Leibowitz, S. G., Nadeau, T-L., 2003. Isolated wetlands: state-of-the-science and future directions. *Wetlands*, 23(3), 663–684.

Loke, M. H.,mBarker, R. D., 1996. Rapid least-squares inversion of apparent resistivity pseudosections by a quasi-Newton method1. *Geophysical Prospecting*, 44(1), 131-152.

McLaughlin, D. L., Kaplan, D. A., Cohen, M. J., 2014. A significant nexus: Geographically isolated wetlands influence landscape hydrology. *Water Resources Research*, 50, 7153–7166. https://doi.org/10.1002/2013WR015002

Milson, J., 1939. *Field Geophysics* – A Handbook of the Geophysical Society of London.

Mitsch, W. J., Gosselink, J. G., 1993. *Wetlands*. Van Nostrand Reinhold.

Neff, B. P., Rosenberry, D. O., Leibowitz, S. G., Mushet, D. M., Golden, H. E., Rains, M. C., Lane, C. R., 2019. A hydrologic landscapes perspective on groundwater connectivity of depressional wetlands. *Water*, 12(1), 50.

Ockenden, M.C., Deasy, C., Quinton, J.N., Surridge, B. Stoate, C., 2014. Keeping agricultural soil out of rivers: Evidence of sediment and nutrient accumulation within field wetlands in the UK. *Journal of Environmental Management*, 135, 54-62.

OECD, 2024. https://www.oecd.org/en.html (10 December 2024).

Pyzoha, J. E., Callahan, T. J., Sun, G., Trettin, C. C., Miwa, M., 2008. A conceptual hydrologic model for a frested Carolina bay depressional wetland on the Coastal Plain of South Carolina, USA. *Hydrological Processes*: An International Journal, 22(14), 2689-2698.

Riley, J. W., Stillwell, C. C., 2023. Predicting inundation dynamics and hydroperiods of small, isolated wetlands using a machine learning approach. *Wetlands*, *43*(6), 63.

Sidle, R. C., Gomi, T., Usuga, J. C. L., Jarihani, B., 2017. Hydrogeomorphic processes and scaling issues in the continuum from soil pedons to catchments. *Earth-Science Reviews*, 175, 75-96.

Steele, M. K., Heffernan, J. B., 2014. Morphological characteristics of urban water bodies: mechanisms of change and implications for ecosystem function. *Ecological Applications*, 24(5), 1070-1084.

Tabari, H., 2021. Extreme value analysis dilemma for climate change impact assessment on global flood and extreme precipitation. *Journal of Hydrology*, 593, 125932.

Thomaz, E. L., Marcatto, F. S., Antoneli, V., 2022. Soil erosion o the Brazilian sugarcane cropping system: An overview. *Geography and Sustainability*, 3(2), 129-138.

Wolka, K., Tadesse, H., Garedew, E., Yimer, F., 2015. Soil erosion risk assessment in the Chaleleka wetland watershed, Central Rift Valley of Ethiopia. *Environmental Systems Research*, 4, 1-12.

Wojkowski, J., Wałęga, A., Młyński, D., Radecki-Pawlik, A., Lepeška, T., Piniewski, M., Kundzewicz, Z. W., 2023. Are we losing water storage capacity mostly due to climate change–Analysis of the landscape hydric potential in selected catchments in East-Central Europe. *Ecological Indicators*, 154, 110913.

Yáñez-Morroni, G., Suárez, F., Muñoz, J. F., Lagos, M. S., 2023. Hydrological modeling of the Silala River basin. 2. Validation of hydrological fluxes with contemporary data. WIREs *Water*. First published: 22 October 2023. https://doi.org/10.1002/wat2.1696

Zaine, J. E., 2000. Mapeamento geológico–geotécnico por meio do método do detalhamento progressivo: ensaio sobre o ambiente dos cordões arenosos da região do Cabo Frio (RJ). *Boletim de Geociências da Petrobras*, 14(2), 253–259.